Topological and magnetic phase transitions in Bi_{2}Se_{3} thin films with magnetic impurities

Hosub Jin, Jino Im, and Arthur J. Freeman

Phys. Rev. B **84**, 134408 — Published 11 October 2011

DOI: 10.1103/PhysRevB.84.134408

Topological and Magnetic Phase Transitions in Bi_2Se_3 Thin Films with Magnetic Impurities

Hosub Jin,[1,*] Jino Im,[1,†] and Arthur J. Freeman[1]

[1] *Department of Physics and Astronomy, Northwestern University, Evanston, Illinois 60208, USA*

When topological insulators meet broken time-reversal symmetry, they bring forth many novel phenomena, such as topological magneto-electric, half quantum Hall, and quantum anomalous Hall effects. From the well-known quantum spin Hall state in Bi_2Se_3 thin films, we predict various topological and magnetic phases when the time-reversal symmetry is broken by magnetic ion doping. As the magnetic ion density increases, the system undergoes successive topological or magnetic phase transitions due to variation of the exchange field and the spin-orbit coupling. In order to identify the topological phases, we vary the spin-orbit coupling strength from zero to the original value of the system and count the number of band crossings between the conduction and valence bands, which directly indicates the change of the topological phase. This method provides a physically intuitive and abstract view to figure out the topological character of each phase and the phase transitions between them.

Newly discovered topological insulators (TI) are differentiated from normal band insulators (BI) by the coexistence of a bulk band gap and gapless edge or surface states at the boundary[1–3]. The odd number of gapless surface states protected by time-reversal symmetry (TRS) show unique features such as spin chirality related to spin-momentum locking[4] and the absence of backscattering by non-magnetic impurities[5], which make TI a promising candidate for spintronics applications. Combined with superconductivity or magnetism, TI have attracted great attention due to the rich variety of new physics and applications made possible; it provides, for example, topological magneto-electric effects[6], majorana zero mode[7], and so on.

The quantum anomalous Hall (QAH) phase characterized by the quantized Hall conductance is another novel insulating phase derived from the combination of TI and magnetism. When the amount of TRS breaking field increases in the TI phase, the exchange field can kill the non-trivial topology of one spin channel whereas the other channel remains as inverted band structures between the conduction and valence bands. Recently, the QAH phase was predicted in HgTe quantum wells, TI thin films, and graphene with magnetic impurities[8–10].

In this work, we uncover the various phases induced by changing the concentration of the magnetic impurity in two-dimensional (2D) TI thin films. In the process of increasing the amount of magnetic dopants, we find magnetically and/or topologically different phases as well as the same phases from 2D TI, the so-called quantum spin Hall (QSH) and QAH states, for which the competition between the exchange field and spin-orbit coupling (SOC) is responsible. In order to identify each phase, we adopt the method proposed in ref[11,12], which studied the topological phase transition by varying external parameters, and expand it to the systems without TRS.

TI undergoes topological phase transitions as the SOC strength increases from 0 up to the real value of the system (λ_0). At the transition point, a crossing between the conduction and valence bands occurs, resulting in the appearance of the Dirac cone in momentum space. The

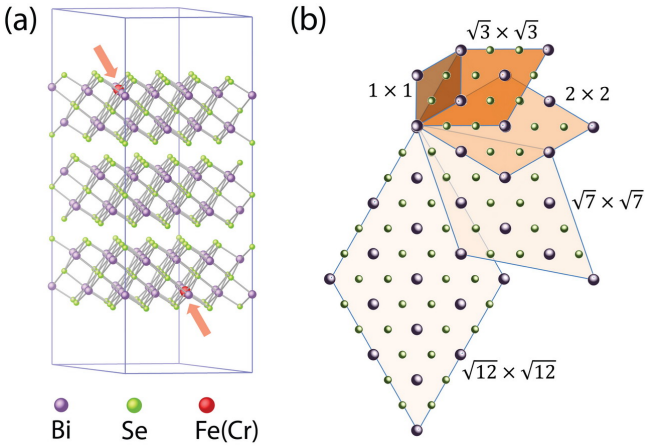

FIG. 1. (Color online) (a) Atomic structure of the 3QL Bi_2Se_3. The red arrow indicates the position of 2 magnetic ions replacing an inversion pair of Bi atoms. (b) Supercell geometries considered in the calculations.

Dirac cone generates magnetic monopole-like Berry curvature, and its monopole charge, from integration of the field over the Brillouin zone, corresponds to the quantized topological number. Due to the TRS, two Kramer's pairs of the conduction and valence bands are involved in the band crossing at the critical SOC strength. Once TRS breaking perturbations are introduced, the Kramer's degeneracy is split and topological phase transitions occur at two different SOC values. By counting the number of band crossing points within the range of the SOC strength from 0 to λ_0 or by tracing the two critical strengths, we can classify the topological and magnetic phases of the system and this is done here.

Bulk Bi_2Se_3 has a rhombohedral crystal structure with space group D^5_{3d} ($R3m$) with five atoms in a unit cell and a layered structure stacked along the c-axis of the hexagonal lattice. One layer composed of five atoms is known as a quintuple layer (QL) and the interlayer coupling is due to the van der Waals interaction. The calculations

are performed with the experimental lattice parameters of bulk Bi_2Se_3 for the in-plane lattice constants and with full relaxation of the c-axis and the internal coordinates. For magnetic doping, magnetic ions substitute for the outermost Bi atoms, and the inversion symmetry of the system is conserved for simplicity (See Fig. 1(a)). To show the various topological phases by changing the exchange field strength, we vary the doping concentration or the atomic species of the magnetic ions (Cr and Fe). Variation of the magnetic ion concentration is determined by varying the supercell size. In Fig. 1(b), 5 different supercells are presented; 1×1, $\sqrt{3}\times\sqrt{3}$, 2×2, $\sqrt{7}\times\sqrt{7}$, and $\sqrt{12}\times\sqrt{12}$ configurations used for simulating the doping concentrations from 2.8% up to 33.3%.

To optimize the geometry, determine the electronic structures, and investigate the topological phase transition in 2D Bi_2Se_3 films, we carried out first-principles electronic structure calculations using planewave basis and pseudopotentials within density functional theory. We employ the projector augmented wave pseudopotential[13] and the local density approximation[14] with on-site Coulomb interaction U[15] as implemented in the Vienna *ab initio* simulation package[16]. For the localized $3d$ orbitals of the magnetic ions, $U_{\rm eff}$ $(=U-J)$ was set equal to 4.0eV. To vary the SOC strength, the radial integral part was multiplied by a simple constant.

One simple way to verify the TI phase is to vary the SOC ratio x $(=\lambda_{\rm SO}/\lambda_0)$ from 0 to 1, where $\lambda_{\rm SO}$ is the SOC strength used in calculations, and to see the band crossing at some critical value x_c smaller or larger than 1, as schematically depicted in Fig. 2(a). The Dirac cones appearing at the phase transition point x_c are doubly degenerate due to TRS. In other words, there are two critical values x_{c_1} and x_{c_2} of the SOC ratio, and they coincide with each other in time-reversal invariant systems. Under the TRS breaking perturbation, such as ferromagnetic long range ordering of the magnetic impurities, two critical values are split, i. e. $x_{c_1}\neq x_{c_2}$ as shown in Fig. 2(b); without loss of generality, we assume that $x_{c_1}\leq x_{c_2}$. The topological phase of the TRS broken system is determined by the relative positions among x_{c_1}, x_{c_2} and 1. If the magnetic perturbation in the QSH phase is small, the splitting between x_{c_1} and x_{c_2} is also small, satisfying the condition $x_{c_1}<x_{c_2}<1$. As a result, a new phase which is adiabatically connected to QSH but exhibits broken TRS emerges. We call the original QSH phase $(x_{c_1}=x_{c_2}<1)$ as QSH with TRS and the new phase $(x_{c_1}<x_{c_2}<1)$ as QSH without TRS. Upon increasing the doping concentrations further, the splitting gets larger, and finally the larger critical value x_{c_2} exceeds 1 $(x_{c_1}<1<x_{c_2})$. This is an another new phase called the QAH insulator[9] which has a level crossing only one time as the SOC ratio x varies from 0 to 1. Across the critical value x_{c_1}, the conduction and valence bands exchange the Chern number equivalent to the quantized Hall conductivity, and the system has a non-trivial band topology[17–19]. Consequently, we expect two successive phase transitions from QSH with TRS to the QSH without TRS phase to the QAH phase by increasing the amount of TRS breaking. The former and the latter correspond to magnetic and topological phase transitions, respectively.

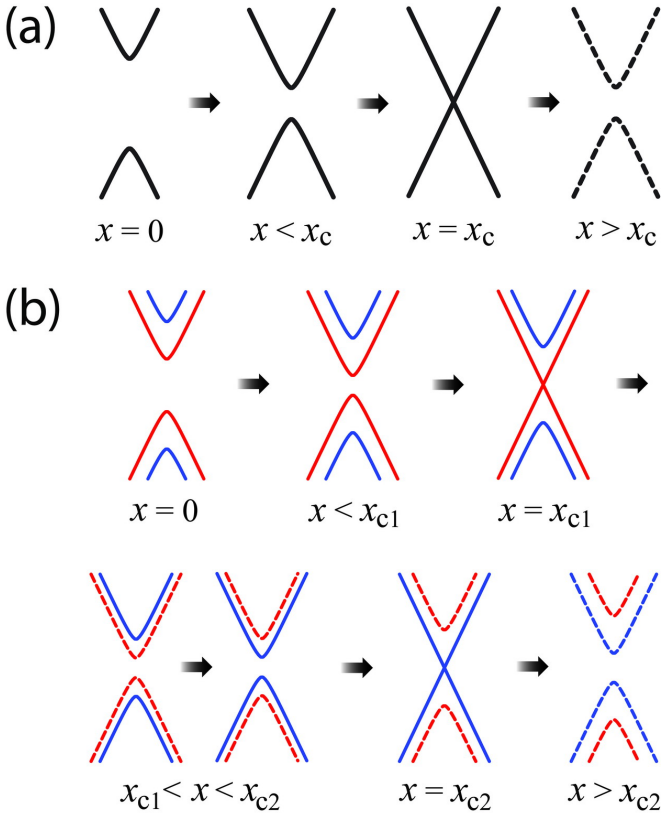

FIG. 2. (Color online) Schematic diagrams of the conduction and valence bands evolving as a function of the SOC ratio x (a) without and (b) with the exchange splitting. Inverted bands induced by increasing the SOC are denoted by dashed lines. (a) Due to TRS, the bands are doubly degenerate, forming a Kramer's pair. Before and after the presence of the Dirac cone at $x=x_c$, the band topology is changed from a trivial to a non-trivial phase. (b) Doubly degenerate bands are split into red and blue bands by the exchange field. Each band undergoes a band crossing at two different critical points x_{c_1} and x_{c_2}, successively.

Bi_2Se_3 is a 3D TI and has a surface state connecting the conduction and valence bands at the boundary[20,21]; one gapless Dirac cone assigned to one surface is protected by TRS. However, in a thin film geometry, the two surfaces are not separated spatially so that the surface state loses its oddness and acquires a mass gap at the Dirac point due to the inter-surface interaction[22]. Therefore, the 3QL Bi_2Se_3 thin film is considered as a 2D insulator with a small gap of 7.8 meV at the Γ point. By varying the SOC ratio from 0 to 1, the electronic structure of the 3QL Bi_2Se_3 slab undergoes a band crossing at x_c=0.965 (<1), as shown in Fig. 3(a). This result indicates that the pristine 3QL Bi_2Se_3 thin film belongs to the QSH phase[23]. Topologically protected 1D con-

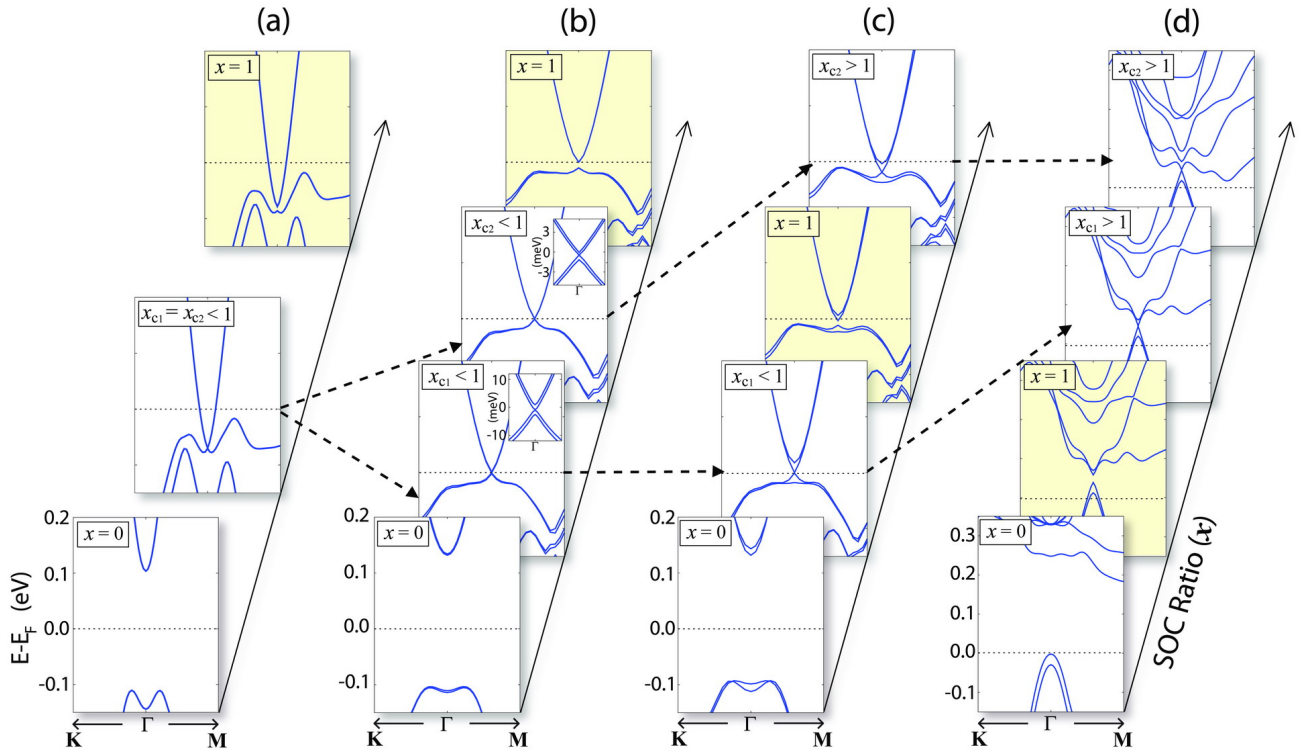

FIG. 3. (Color online) Band structures of the 3QL Bi_2Se_3 slab as a function of the SOC ratio x in (a) the pristine case, (b) 2.8% Cr-doping, (c) 2.8% Fe-doping, and (d) 33.3% Fe-doping. The critical values of the SOC ratio are directly examined by gap closing: (a) $x_{c_1} = x_{c_2} = 0.965$ for the pristine case, (b) $x_{c_1} = 0.944$ and $x_{c_2} = 0.949$ for 2.8% Cr-doping, (c) $x_{c_1} = 0.878$ and $x_{c_2} = 1.055$ for 2.8% Fe-doping, and (d) $x_{c_1} = 1.063$ and $x_{c_2} = 1.252$ for 33.3% Fe-doping. Each configuration corresponds to (a) QSH with TRS, (b) QSH without TRS, (c) QAH, and (d) trivial FM phase, respectively. The evolution of the critical values are guided by the black dashed arrow. Insets of (b) are enlarged pictures near the Dirac point at two critical values.

ducting edge states are expected at the 1D boundary of Bi_2Se_3 and the BI[24,25]. 3QL Bi_2Se_3 thin film is a good starting point to obtain the QAH phase in terms of its topological phase, gap, and x_c close to 1.

Since the critical SOC ratio is quite close to 1, the 3QL Bi_2Se_3 thin film is located in the vicinity of the topological phase boundary, and it is expected that its topological phase is easily tuned by small perturbations. The QSH without TRS phase is realized in the 2.8% Cr doped 3QL Bi_2Se_3 film. As shown in Fig. 3(b), the band crossing between the conduction and valence bands occurs at $x = 0.944$ and 0.949. The small difference between x_{c_1} and x_{c_2} indicates the small exchange splitting in conduction and valence bands from the d-p hybridization with the Cr impurities. The magnetic moment per Cr atom is nearly $3\mu_B$ and aligned along the c-axis, and the exchange splitting of the conduction band at the Γ point is 2.3 meV without SOC. QSH with and without TRS phases are connected by continuous deformation of the electronic band structures without gap closing. The adiabatic connection between the two QSH phases guarantees that the number of edge states is the same. However, even though there are two counter-propagating edge states in the QSH without TRS phase, they are no longer time-reversal partners.

By maintaining the doping concentration but changing atomic species of Cr by Fe, we are able to increase the ferromagnetic moment by $5\mu_B$ per Fe atom aligned along the c-axis and the exchange splitting by 11.6 meV at the Γ point without SOC. Consequently, the QAH phase indicated by the condition $x_{c_1} < 1 < x_{c_2}$ is realized in Fig. 3(c) ($x_{c_1} = 0.878$ and $x_{c_2} = 1.055$). Because x_{c_2}, the second band crossing point, passes through 1 as the QSH evolves into the QAH phase when the exchange field grows, continuous deformation between the two phases without closing a gap is impossible, and the topological phase transition takes places. The QAH phase prevails over the range from 2.8% to 16.6% Fe doping in the 3QL Bi_2Se_3 slab, and the bandgaps of the QAH phase are distributed from 6.9 meV (2.8%) to 39.1 meV (11.1%)[26].

Upon increasing the Fe density further, the system undergoes another topological phase transition; the 33.3% Fe doped 3QL Bi_2Se_3 film shows two critical values larger than 1 as shown in Fig. 3(d) ($x_{c_1} = 1.063$ and $x_{c_2} = 1.252$), designating the trivial ferromagnetic (FM) phase. Because there is no band crossing during the growth of the SOC ratio from 0 to 1, the electronic structure with full SOC strength is adiabatically connected to the $x = 0$ state which has a trivial topology. From QAH to trivial FM, the number of critical values smaller than

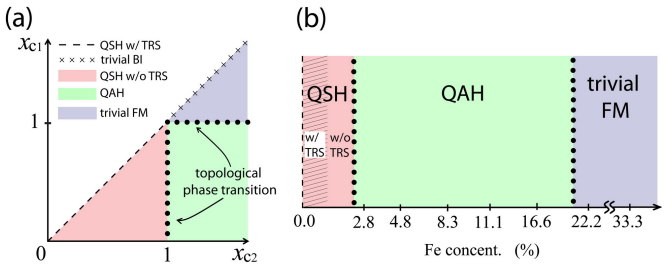

FIG. 4. (Color online) (a) Classification of each magnetic and topological phase in the (x_{c_1}, x_{c_2}) plane and (b) the phase diagram on the 3QL Bi_2Se_3 slab. In (a), QSH with TRS, QSH without TRS, QAH, trivial FM, and BI phases are plotted as a function of critical values of the SOC ratio. In (b), QSH with TRS, QSH without TRS, QAH, and trivial FM phases are shown as the extent of magnetic doping increases.

1 is altered; thus, the transition is identified as a topological phase transition. This topological phase transition is not related to the increase of the exchange field, but is induced by the decrease of the SOC strength because Fe has a much smaller SOC strength than Bi. Once we increase the doping concentration, the SOC strength of the system λ_0 decreases simultaneously, making the first critical value x_{c_1} larger than 1. To see the effect of the reduced SOC strength with excluding the influence of the exchange field, we calculated the hypothetical structure where every Fe atom in the trivial FM phase is replaced by As. The As-replaced system shows a trivial BI phase, i. e. two degenerate critical SOC ratios exceed 1, and this is indirect evidence that the QAH to trivial FM transition is mainly driven by reduction of the SOC strength.

Various phases identified by the range of the two critical SOC ratios, x_{c_1} and x_{c_2}, are sketched in Fig. 4(a). In this diagram, we assume that all phases, except for the critical line where the topological phase transition occurs ($x_{c_1} = 1$ or $x_{c_2} = 1$), are gapped and TRS is broken by the ferromagnetic ordering. Now the x_c's are proportional to $\Delta_{\rm gap}/\lambda_0$ where $\Delta_{\rm gap}$ is a bulk gap without SOC, and the difference between x_{c_1} and x_{c_2} is proportional to the exchange field. Therefore, the system with the SOC strength comparable to $\Delta_{\rm gap}$ and a moderate magnetic ion doping might be located around $x_{c_1} = x_{c_2} = 1$ where the five different phases overlap, and easily show successive phase transitions by a small external perturbation.

The phase diagram of the 3QL Bi_2Se_3 thin film as a function of Fe concentration is depicted in Fig. 4(b). Upon increasing the Fe content, a magnetic phase transition occurs within the QSH phase, and then two topological phase transitions from QSH to QAH, and from QAH to trivial FM follow. The driving force for the first two transitions is the increase of the exchange field and the last one originates from the reduced SOC strength. From the competition between the exchange splitting and the SOC strength, the QAH phase is bounded, and the phase boundary is located near the 22.2% Fe doping concentration whose x_{c_1} is very close to 1 ($x_{c_1} = 1.005$). The shaded area of the QSH with TRS phase considers the onset of ferromagnetic long range ordering of the Fe impurities, which seems easily accessible according to the previous study[9,27].

We presented various topological and magnetic phases and the transitions between them in the 3QL Bi_2Se_3 thin film with magnetic impurities. Each phase is described by means of two critical SOC ratios, which provide intuitive understanding of the topological phase transition accompanied by the magnetic transition. Because the topological phases of the 2D systems are directly related to the existence and the character of the conducting edge states, it would be interesting to investigate the evolution of the edge states as the amount of the magnetic ion doping changes. In the QAH phase, the propagating direction of the edge state carrying the quantized Hall currents are coupled to the direction of the ferromagnetic moments of the magnetic impurities. Thus the Hall currents are able to be manipulated by flipping the ferromagnetic moments using an external magnetic field. Moreover, the 2D heterostructure or the multi-domain structures containing different Fe densities could show a rich variety of interesting features, such as various topological phase domains and the conducting boundary states, and they might be applicable to electronic and spintronic devices using various 1D conducting channels.

ACKNOWLEDGMENTS

Support from the U.S. DOE under Grant No.DE-FG02-88ER45372 is gratefully acknowledged.

* h-jin@northwestern.edu
† j-im@northwestern.edu

[1] M. Z. Hasan and C. L. Kane, Rev. Mod. Phys. **82**, 3045 (2010).
[2] X. L. Qi and S. C. Zhang arXiv:1008.2026v1.
[3] J. E. Moore, Nature **464**, 194 (2010).
[4] D. Hsieh *et al.*, Nature **460**, 1101 (2009).
[5] P. Roushan *et al.*, Nature **460**, 1106 (2009).
[6] X.-L. Qi, R. Li, J. Zang, and S.-C. Zhang, Science **323**, 1184 (2009).
[7] L. Fu and C. L. Kane, Phys. Rev. Lett. **100**, 096407 (2008).
[8] C.-X. Liu *et al.*, Phys. Rev. Lett. **101**, 146802 (2008).
[9] R. Yu *et al.*, Science **329**, 61 (2010).
[10] Z. Qiao *et al.*, Phys. Rev. B **82**, 161414 (2010).
[11] S. Murakami and S.-i. Kuga, Phys. Rev. B **78**, 165313 (2008).
[12] H. Jin, J.-H. Song, A. J. Freeman, and M. G. Kanatzidis, Phys. Rev. B **83**, 041202 (2011).
[13] P. E. Blöchl, Phys. Rev. B **50**, 17953 (1994).
[14] D. M. Ceperley and B. J. Alder, Phys. Rev. Lett. **45**, 566

(1980).
[15] A. I. Liechtenstein, V. I. Anisimov, and J. Zaanen, Phys. Rev. B **52**, R5467 (1995).
[16] G. Kresse and J. Furthmüller, Phys. Rev. B **54**, 11169 (1996).
[17] D. J. Thouless, M. Kohmoto, M. P. Nightingale, and M. den Nijs, Phys. Rev. Lett. **49**, 405 (1982).
[18] J. E. Avron, R. Seiler, and B. Simon, Phys. Rev. Lett. **51**, 51 (1983).
[19] In these inversion-symmetric systems, conduction and valence bands exchange their parities at the crossing point.
[20] Y. Xia *et al.*, Nature Phys. **5**, 398 (2009).
[21] H. Zhang *et al.*, Nature Phys. **5**, 438 (2009).
[22] Y. Zhang *et al.*, Nature Phys. **6**, 584 (2010).
[23] C.-X. Liu *et al.*, Phys. Rev. B **81**, 041307 (2010).
[24] C. L. Kane and E. J. Mele, Phys. Rev. Lett. **95**, 226801 (2005).
[25] M. König *et al.*, Science **318**, 766 (2007).
[26] Our system is composed of 3QL Bi_2Se_3 which is in the ultathin limit and can be considered close to the 2-dimensional objects. The conduction and valence bands in these thin films, which are originally the two surface states from each surface spread over the 3QL. In the 11.1% doping configuration, we have checked the position dependence of the Fe dopants, and still found out the QAH phase for all three different locations. It is expected that the position dependence of the magnetic ions might be crucial for the thick film geometry. Considering the 2-3nm spread of the surface states, the position dependence might emerge above 5 or 6QL films.
[27] L. A. Wray *et al.*, Nature Phys. **7**, 32 (2011).